FRICTION COMPENSATION IN A CONTROLLED ONE-LINK ROBOT USING A REDUCED-ORDER OBSERVER

Nathan van de Wouw * **Niels Mallon**
Henk Nijmeijer

* *Eindhoven University of Technology*
Department of Mechanical Engineering
P.O. Box 513, 5600 MB, Eindhoven, The Netherlands,
email: N.v.d.Wouw@tue.nl, N.J.Mallon@tue.nl,
H.Nijmeijer@tue.nl

Abstract: Friction compensation in a controlled one-link robot using a reduced-order observer is studied. Since friction is generally velocity-dependent and controlled mechanical systems are often only equipped with position sensors, friction compensation requires velocity estimation. Here, a reduced-order linear observer is used for this purpose. For exact friction compensation, design criteria in terms of the controller and observer parameter settings guaranteeing global exponential stability of the set-point are proposed. Moreover, for non-exact friction compensation it is shown that undercompensation leads to the existence of an equilibrium set and overcompensation leads to limit cycling. These results are obtained both numerically and experimentally.

Keywords: Friction compensation, reduced-order observers, discontinuous mechanical systems, stability, differential inclusions, bifurcations.

1. INTRODUCTION

The positioning performance of many controlled mechanical systems, such as robots and optical disc drives, is limited by the presence of dry friction (Armstrong-Hélouvry, 1991; Olsson *et al.*, 1998). For example friction-induced limit cycling is observed by many authors in controlled mechanical systems (Armstrong-Hélouvry *et al.*, 1994; Armstrong-Hélouvry and Amin, 1996; Hensen, 2002). One possible strategy to tackle this problem is model-based friction compensation. In the literature, friction compensation is investigated in both a feedforward (the friction compensation is based on desired variables) and a feedback manner (the friction compensation is based on actual variables) (Armstrong-Hélouvry, 1991; Johnson and Lorenz, 1991; Olsson *et al.*, 1998; Armstrong-Hélouvry *et al.*, 1994). Here, we will apply a feedback friction compensation strategy to a controlled one-link robot in order to enhance its positioning performance.

In order to implement such a strategy, a model of the friction and knowledge on the variables on which the friction model depends is needed. Based on experiments, a friction model depending on velocity is adopted here. Furthermore, a linear proportional-derivative controller is used. Since only position measurements are available for the one-link robot (and for mechanical systems in general), some form of velocity estimation is required. To this end, numerical differentiation of the position measurements (Wang *et al.*, 2000) or an observer can be used (Friedland and Mentzelopoulou, 1992; Putra and Nijmei-

jer, 2004). Here, we opt for an observer, since numerical differentiation is very sensitive to measurement noise.

The combination of dry friction, friction compensation and the observer dynamics can give rise to undesired phenomena, such as limit cycling (Putra and Nijmeijer, 2004) and the existence of equilibrium sets. The existence of equilibrium sets are due to discontinuities in the friction and friction compensation and can cause a non-zero steady-state positioning error. Consequently, improved insight into the influence of controller and observer design parameters on the existence of these unwanted phenomena is needed. Here, a combination of a reduced-order linear observer and a PD-controller will be used. This combination exhibits only three design parameters (two controller gains and one observer gain), which allows for a simplified analysis of the effect of these parameters on the behaviour of the closed-loop system.

This analysis provides design criteria for the parameters of the controller and observer, which ensure the avoidance of unwanted behaviour such as limit cycling and equilibrium sets, in the case of exact friction compensation. These criteria are based on a stability analysis of the set-point. The approach proposed here can be extended towards multi-degree-of-freedom systems. Moreover, the influence of non-exact friction compensation on the positioning performance is investigated numerically as well as experimentally.

The paper is organized as follows. In Section 2, the experimental setup and a corresponding model is introduced, based on experiments. The controller design, observer design and the adopted friction compensation strategy are discussed in Section 3. In Section 4, the dynamic behaviour of the system in case of exact friction compensation is investigated and design criteria for the controller and observer are proposed such that the set-point is globally exponentially stable. Moreover, in Section 5, the effect of non-exact friction compensation on the positioning performance is investigated both numerically and experimentally. Finally, in Section 6 conclusions are presented.

2. EXPERIMENTAL SET-UP AND MODELLING

The experimental setup involving the one-link robot is depicted schematically in figure 1. The link is driven by a (control)-torque u supplied by an induction motor. The angular position q is measured by a position encoder.

The robot is modelled as a single inertia J (modelling the inertia of the link and the driveline) subject to a viscous friction torque $-b\dot{q}$, a dry

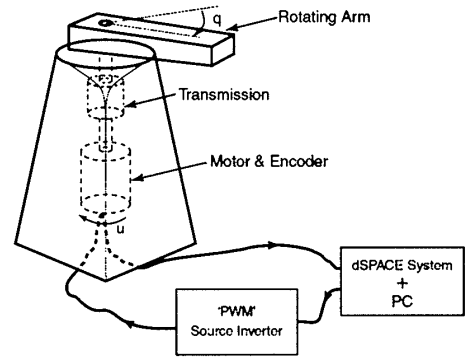

Figure 1: The Experimental Setup.

friction torque $-F_f(\dot{q})$ and a control torque u, which leads to the following model:

$$J\ddot{q} + b\dot{q} = u - F_f(\dot{q}). \tag{1}$$

Using a frequency-domain identification technique, the total inertia of the system is identified to be $J = 0.026$ kgm^2/rad.

In order to identify the dry friction model, breakaway experiments are performed to measure the static friction torque and constant velocity experiments are performed to measure the friction torque at non-zero (constant) velocities. A set-valued force law expressed by the following algebraic inclusion is used:

$$F_f(\dot{q}) \in g(\dot{q})\mathrm{Sign}(\dot{q}), \tag{2}$$

in which $g(\dot{q})\mathrm{Sign}(\dot{q})$ represents the Stribeck curve including the modelling of stiction, with

$$g(\dot{q}) = F_c + \delta F e^{-\left(\frac{|\dot{q}|}{v_s}\right)^{\beta}} \tag{3}$$

and $\mathrm{Sign}(x)$ the set-valued sign-function:

$$\mathrm{Sign}(x) = \begin{cases} \{-1\} & x < 0 \\ [-1, 1] & x = 0 \\ \{1\} & x > 0 \end{cases}. \tag{4}$$

Herein, F_c is the Coulomb friction force, δF the difference between the static and Coulomb friction force ($\delta F = F_s - F_c$), v_s the Stribeck velocity and β the Stribeck shape parameter. The measurement results and the friction model (including both viscous and dry friction) fitted to these data are displayed in figure 2. The resulting friction parameter estimates are given in table 1, where different parameter estimates are obtained for positive and negative velocities indicating an asymmetric friction model. For the remainder of this paper a symmetric friction model will be used, since the asymmetry is not essential in the analysis. The friction parameters used in this symmetric model are the mean values of those for positive and negative velocity, see table 1.

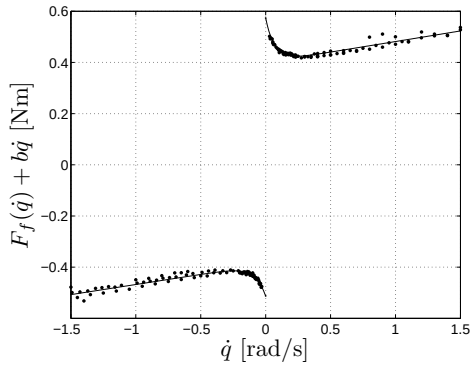

Figure 2: Friction measurements (dots) and friction model (solid line).

parameter	$\dot{q} > 0$	$\dot{q} < 0$	mean value
β [-]	1	1	1
F_s [Nm]	0.5735	0.5123	0.5429
F_c [Nm]	0.3990	0.3887	0.3939
v_s [rad/s]	0.0688	0.0817	0.0753
b [Nms/rad]	0.0828	0.0790	0.0809

Table 1: Friction parameter estimates.

3. CONTROLLER DESIGN, OBSERVER DESIGN AND FRICTION COMPENSATION STRATEGY

In figure 3, the friction compensation strategy incorporating the reduced-order linear observer and a proportional-derivative controller is depicted schematically. The total control action u is composed by the feedback control u_c and the friction compensation u_{fc}: $u = u_c + u_{fc}$. Herein,

$$u_c = n_1(q_r - q) - n_2\hat{\dot{q}}, \tag{5}$$

where $n_1, n_2 > 0$ are the proportional gain and the derivative gain, respectively, and $\hat{\dot{q}}$ is the velocity estimate provided by the observer. Moreover, q_r is the desired reference position, which will be assumed to equal zero (without loss of generality). Furthermore, the following set-valued friction compensation law is adopted

$$u_{fc} = rF_f(\hat{\dot{q}}) \in rg(\hat{\dot{q}})\mathrm{Sign}(\hat{\dot{q}}), \tag{6}$$

where r is a scaling factor of the friction compensation. Clearly, it reflects a feedback compensation strategy where the estimated velocity is provided by an observer. When $r = 1$, exact friction compensation is attained and, when $r \neq 1$, non-exact friction compensation is attained.

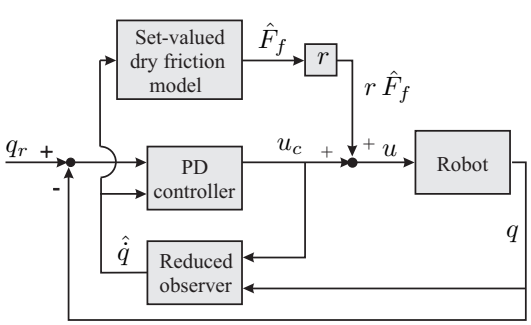

Figure 3: Friction compensation strategy.

The reduced-order observer is designed as

$$\dot{\hat{\dot{q}}} = -\frac{b}{J}\hat{\dot{q}} + \frac{1}{J}(u - u_{fc}) + L\left(\dot{q} - \hat{\dot{q}}\right), \tag{7}$$

where $\hat{\dot{q}}$ is the observer state (the velocity estimate) and $L > 0$ is the observer gain. The observer error is defined as $e = \dot{q} - \hat{\dot{q}}$.

From now on, we will adopt the state coordinates $\boldsymbol{x} = \left[q\ \hat{\dot{q}}\ e\right]^T$. The dynamics of the closed-loop system, displayed in figure 3, can be formulated in terms of these states by the following differential inclusion:

$$\begin{aligned} \dot{x}_1 &= x_2 + x_3 \\ \dot{x}_2 &= -\frac{n_1}{J}x_1 - \frac{b+n_2}{J}x_2 + Lx_3 \\ \dot{x}_3 &\in -\frac{b+LJ}{J}x_3 + \frac{1}{J}\left[rF_f(x_2) - F_f(x_2+x_3)\right]. \end{aligned} \tag{8}$$

The differential inclusion (8) is of Filippov-type and thus obeys Filippov's solution concept (Filippov, 1988). Consequently, the existence of solutions of system (8) is guaranteed.

4. EXACT FRICTION COMPENSATION

In this section, the behaviour of the closed-loop system is investigated for the case of exact friction compensation. i.e. $r = 1$ in (6). First, the existence of an equilibrium set depending on the system (and control) parameters is discussed. Second, the stability of the set-point (the origin) is investigated.

4.1 Equilibria

The equilibria of (8) satisfy the following equations and inclusion:

$$\begin{aligned} x_2 &= -x_3 \\ x_1 &= -\frac{LJ + b + n_2}{n_1}x_2, \\ G(x_2) &\in [-F_s, F_s] \end{aligned} \tag{9}$$

where

$$G(x) = (b + LJ)x + F_f(x). \tag{10}$$

Let us denote these equilibria by $\boldsymbol{x}^*$. The origin is always an equilibrium. However, depending on the observer gain L an equilibrium set exists. In figure 4, the equilibria of the system with exact friction compensation are compared to those of the system with no compensation. In this figure, the effect of the existence the equilibrium set on the steady-state positioning error x_1 is depicted, for $n_1 = 0.4$ and $n_2 = 0.02$ and for varying L. Clearly, the equilibrium set can induce a non-zero steady-state positioning error. However, friction compensation ensures a large decrease in the size

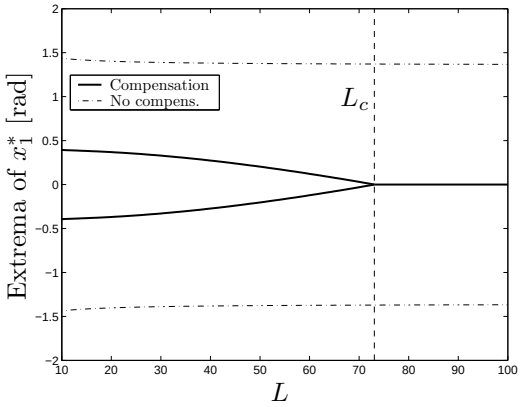

Figure 4: Extrema for steady-state error in x_1 for $n_1 = 0.4$ and $n_2 = 0.02$.

of the equilibrium set. Moreover, in case of exact compensation the equilibrium set shrinks to an isolated equilibrium point for increasing observer gain at some critical value of the observer gain. In order to derive the condition for L such that a single equilibrium point exist we note that $\lim_{x\downarrow 0} G(x) = F_s$ and $\lim_{x\uparrow 0} G(x) = -F_s$. Taking into account the strictly decreasing nature of $F_f(x)$ for $x \neq 0$, a sufficient and necessary condition, under which no equilibrium set can exist, is that the function $G(x)$ is strictly increasing for all $x \neq 0$ (see inclusion in (9)). This is attained if $\frac{\partial}{\partial x}G(x) > 0\ \forall x \neq 0$ and, consequently, if $L > L_c$ where

$$L_c = \frac{1}{J}\left(-\lambda - b\right), \tag{11}$$

$$\lambda = -\frac{\eta\delta F}{v_s} = \min_{x\in\mathbb{R}\setminus\{0\}}\left(\frac{\partial g(x)}{\partial x}\right), \tag{12}$$

and

$$\eta = \begin{cases} 1 & \text{if } \beta = 1 \\ \dfrac{(\beta-1)e^{-\frac{\beta-1}{\beta}}}{\sqrt[\beta]{\frac{\beta-1}{\beta}}} & \text{if } \beta > 1 \end{cases}. \tag{13}$$

For the parameters of the model of the one-link robot (using mean values for the friction parameters) the critical observer gain is $L_c = 73.07$. Note that this value corresponds to the value for which the equilibrium set merges into an isolated equilibrium point in figure 4. The size of the equilibrium set (and thus the maximum steady-state positioning error) can also be influenced by the controller parameters; if n_1 is increased the size of the equilibrium set decreases and if n_2 is increased the size of the equilibrium set increases, see the second equation of (9).

4.2 Stability of the set-point

In order to investigate the stability of the origin of (8), let us study the system in the form of a cascade of a subsystem S_I and a subsystem S_{II} as depicted in figure 5. In this figure, $\boldsymbol{x}_{12} = \left[x_1\ x_2\right]^T$ and the system and input matrices of these subsystems are given by

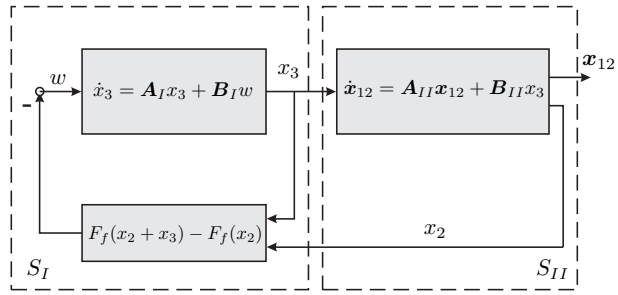

Figure 5: Cascade representation of the closed-loop system.

$$\boldsymbol{A}_I = -(\frac{b}{J} + L), \quad \boldsymbol{B}_I = \frac{1}{J}$$
$$\boldsymbol{A}_{II} = \begin{bmatrix} 0 & 1 \\ -\dfrac{-n_1}{J} & -\dfrac{b+n_2}{J} \end{bmatrix}, \quad \boldsymbol{B}_{II} = \begin{bmatrix} 1 \\ L \end{bmatrix}. \tag{14}$$

Note that S_I describes the observer error dynamics. In order to prove the global exponential stability (GES) of the origin of (8) we adopt the following reasoning. If the following three conditions are fulfilled:

(a) $x_3 = 0$ is a globally exponentially stable equilibrium point of system S_I for all x_2;
(b) $\boldsymbol{x}_{12} = \boldsymbol{0}$ is a globally exponentially stable equilibrium point of system S_{II} for zero input x_3;
(c) System S_{II} is input-to-state stable (ISS),

then $\boldsymbol{x} = \boldsymbol{0}$ is a globally exponentially stable equilibrium point of (8). Let us now check whether these conditions are fulfilled.

Firstly, in order to check condition **(a)**, we use a candidate Lyapunov function $V = \frac{1}{2}Jx_3^2$ (see (Filippov, 1988) and (Shevitz and Paden, 1994) for details on Lyapunov analysis for differential inclusions). Its time-derivative $\dot{V} = J\dot{x}_3x_3$ obeys

$$\dot{V} \in -(b+LJ)x_3^2 + (F_f(x_2) - F_f(x_2+x_3))\,x_3. \tag{15}$$

In the second term of $\dot{V}$ the discontinuities of both the dry friction torque and the friction compensation design are present. Here, we will estimate this term by realising that the function $F_f(\cdot)$ satisfies the following incremental sector condition:

$$(F_f(x_2) - F_f(x_2+x_3))\,x_3 \leq -\lambda x_3^2,\ \forall x_2, x_3 \tag{16}$$

with λ defined by (12). Using (16) in (15) yields

$$\dot{V} \leq -\frac{2}{J}\left(LJ + b + \lambda\right)V. \tag{17}$$

Clearly, for an observer gain satisfying $L > L_c$, with the critical observer gain L_c given by (11), $e = 0$ is a globally exponentially stable equilibrium point of system S_I (independent of x_2).

Secondly, conditions **(b)** and **(c)** are satisfied since system S_{II} is a LTI-system with a Hurwitz

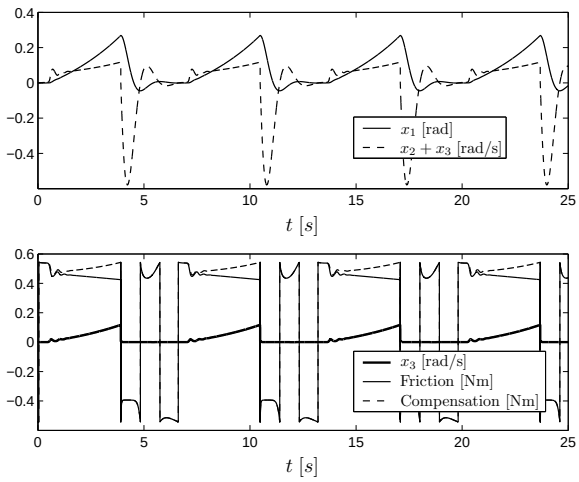

Figure 6: Limit cycle for $L = 40 < L_c$, $n_1 = 0.4$ and $n_2 = 0.02$.

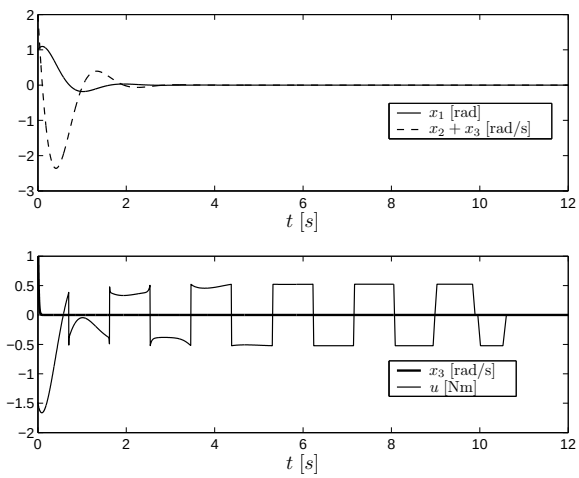

Figure 7: Performance for $L = 73.5 > L_c$, $n_1 = 0.4$ and $n_2 = 0.02$.

system matrix A_{II} (A_{II} is Hurwitz given the fact that $n_1, n_2 > 0$).

Resuming we can conclude that if $L > L_c$, $\boldsymbol{x} = \mathbf{0}$ is a globally exponentially stable equilibrium point of (8). If $L < L_c$, unwanted behaviour in the form of a non-zero steady-state positioning error, see figure 4, or limit cycling, see figure 6, can occur. The latter figure indicates that $e = 0$ is not stable, which causes a non-zero observer error. This non-zero observer error induces overcompensation leading to limit cycling. For $L > L_c$, the observer error converges fast to zero and stays equal to zero, see figure 7. The observer based friction compensation now performs as desired. Note that we used a switch-model (Leine, 2000) for the numerical integration of (8) to avoid numerical instability at zero velocity.

5. NON-EXACT-FRICTION COMPENSATION

In practice, or in an experimental setup such as that of the one-link robot discussed in this paper, the friction model will never be exact, due to inevitable modelling errors. To study this we

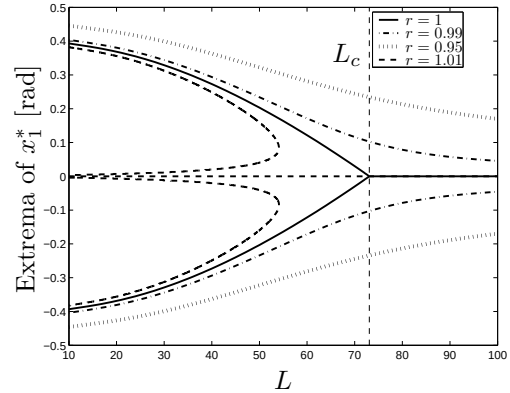

Figure 8: Extrema for steady-state error in x_1 for $n_1 = 0.4$, $n_2 = 0.02$ and various values for r.

introduce a scaled friction compensation law, see figure 3 and equation (6) with $r \neq 1$. Obviously, in practice modelling errors will not be of this form but this type of scaling of the friction compensation law allows to investigate the effects of both undercompensation and overcompensation of the friction. In figure 8, the equilibrium set (in terms of x_1) is shown for different values of r. In the case of undercompensation ($r < 1$), an equilibrium set will exist irrespective of the value of L. The value of L, however, influences the magnitude of the equilibrium set. This figure indicates that friction compensation (even in the case of undercompensation) ensures a smaller equilibrium set than exists without compensation, see also figure 4. In the case of the overcompensation ($r > 1$), an equilibrium set only exists for r very close to one; the equilibrium set rapidly shrinks to an isolated (unstable) equilibrium point for increasing r.

In figure 9, a bifurcation diagram with bifurcation parameter r is depicted in terms of x_1 for a supercritical observer gain $L = 73.5 > L_c$. For the limit cycle, $max(abs(x_1))$ over a period of the limit cycle is plotted. This bifurcation diagram clearly shows that an equilibrium set exists when the friction is undercompensated and a stable limit cycle exists in case of overcompensation. A corresponding bifurcation diagram involving ex-

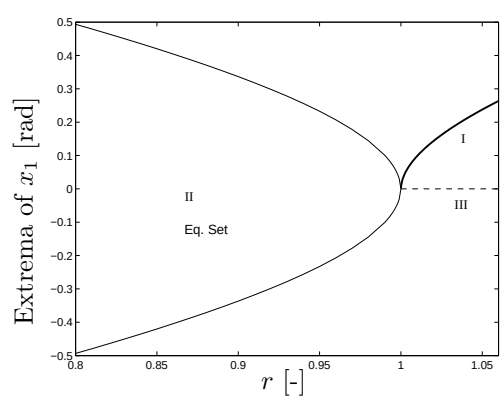

Figure 9: Bifurcation diagram for $n_1 = 0.4$, $n_2 = 0.02$, $L = 73.5$ ((I): Stable limit cycle, (II): Equilibrium set and (III): Unstable equilibrium point.

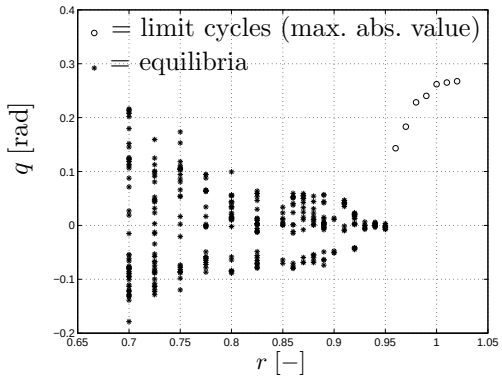

Figure 10: Experimental bifurcation diagram with bifurcation parameter r.

perimental results is depicted in figure 10. Herein, the stars ($*$) indicated equilibria and the circles ($\circ$) indicate limit cycles. Comparison of figures 9 and 10 reveals a clear qualitative correspondence. Of course, in figure 10 the bifurcation point is not located exactly at $r = 1$ since not only the friction compensation law is scaled but the real friction deviates from the friction model as well. Moreover, the difference between the real friction and the friction model is not of the form of a mere scaling. Nevertheless, the theoretical and experimental results agree to the extent that undercompensation leads to non-zero steady-state errors (due to the existence of an equilibrium set) and overcompensation leads to limit cycling.

6. CONCLUSIONS

A friction compensation strategy for a controlled one-link robot using a reduced-order observer is proposed. Based on experiments, a set-valued friction model is identified to support a model-based friction compensation approach. Since only position measurements are available and the friction model depends on velocity, a reduced-order observer is used to provide velocity estimates. The combination of the reduced-order observer and a PD-controller exhibits only three design parameters (two controller gains and one observer gain). This allows for a simplified analysis of the effect of these parameters on the behaviour of the closed-loop system.

Both the case of exact friction compensation and non-exact friction compensation are studied. In the case of exact friction compensation, it is shown that the observer gain is critical for the stability of the set-point. If the observer gain is taken larger than this critical value, it is shown the set-point is globally exponentially stable. Moreover, for an observer gain lower than this critical value, an equilibrium set can exist and limit cycling can occur both deteriorating the positioning performance. In the case of non-exact friction compensation, it is shown that undercompensation of the friction leads to the existence of an equilibrium set and that overcompensation leads to limit cycling. These results are obtained both in simulation and experiments. Since the size of the equilibrium set can be influenced by the choice of the controller parameters, it is advisable to opt for undercompensation when exact friction compensation is not possible.

REFERENCES

Armstrong-Hélouvry, B. (1991). *Control of machines with friction*. Kluwer Academic Publishers. New York.

Armstrong-Hélouvry, B. and B. Amin (1996). Pid control in the presence of static friction: A comparison of algebraic and describing function analysis. *Automatica* **32**, 679–692.

Armstrong-Hélouvry, B., P. Dupont and C. Canudas de Wit (1994). A survey of models, analysis tools, and compensation methods for the control of machines with friction. *Automatica* **30**, 1083–1138.

Filippov, A. F. (1988). *Differential Equations with Discontinuous Right-hand Sides*. Kluwer Academic. Dordrecht.

Friedland, B. and S. Mentzelopoulou (1992). On adaptive friction compensation without velocity measurement. In: *Proc. of the 1st IEEE Conf. on Control Applications*. Dayton, OH. pp. 1076–1081.

Hensen, R. H. A (2002). Controlled Mechanical Systems with Friction. Ph.D. thesis. Eindhoven University of Technology. The Netherlands.

Johnson, C.T. and R.D. Lorenz (1991). Experimental identification of friction and its compensation in precise, position controlled mechanisms. In: *Proc. of the Indus. App. Soc. Annual Meeting*. pp. 1400–1406.

Leine, R.I. (2000). Bifurcations in discontinuous mechanical systems of Filippov type. PhD thesis. Eindhoven University of Technology. The Netherlands.

Olsson, H., K.J. Åström, C. Canudas de Wit, M. Gäfvert and P. Lischinsky (1998). Friction models and friction compensations. *European Journal of Control* **4**(3), 176–195.

Putra, D. and H. Nijmeijer (2004). Limit cycling in an observer-based controlled system with friction: Numerical analysis and experimental validation. *Int. J. of Bifurcation and Chaos* **14**(9), to appear.

Shevitz, D. and B. Paden (1994). Lyapunov stability theory of nonsmooth systems. *IEEE Trans. on Automatic Control* **39**(9), 1910–1914.

Wang, Z., H. Melkote and F. Khorrami (2000). Robust adaptive friction compensation in servo-drives using position measurements only. In: *Proc. of the int. conf. on control applications*. Achorage. pp. 178–183.